24th COBEM - 2017

24th ABCM International Congress of Mechanical Engineering
December 3-8, 2017, Curitiba, PR, Brazil

COBEM-2017- 2570
ANALYSIS OF TORQUE IN FRICTION STIR WELDING BY INVERSE PROBLEM METHOD

Karen J. Quintana
Jose Luis Silveira
Universidade Federal do Rio de Janeiro, Department of Mechanical Engineering, RJ, Brazil
kjq.cuellar@mecanica.coppe.ufrj.br
jluis@mecanica.ufrj.br

Abstract. *Friction Stir Welding (FSW) is a solid state process with several advantages over conventional welding techniques due to the absence of melting and a small energy requirement. Torque is an important quantity in friction stir welding as it influences the main phenomena that occur during the process. However, studies of torque behavior in FSW have received little attention. In this paper, inverse problem method is used to estimate the parameters for an experimental model for torque. The torque was measured during FSW experiments for different combinations of rotational and welding speeds. The experimental results were used as input data to estimate the model parameters. The results showed a good agreement between the experimental data and the model obtained using the inverse problem method.*

Keywords: *Friction Stir Welding, Torque behavior, model optimization, FSW experiments, Inverse problem.*

1. INTRODUCTION

Friction stir welding (FSW) is an alternative to the conventional fusion welding mainly developed to weld materials with poor weldability such as aluminum, magnesium, copper, and other light alloys (Mishra and Ma, 2005; Rajakumar *et al*., 2011). In the FSW process, the friction at the surface of the tool due to the tool rotation produces localized heating that softens the material around the tool. The softened material is plastically deformed when the tool rotation stirs the material to produce the joint. Therefore, the quality of the welded joint is better than in the most widely used welding methods, the FSW process reduces defect formation, is cost-efficient, and is easy to process (Rhodes *et al*., 1997; Qian, 2013; Long *et al.,* 2007)

The torque in the FSW process is related to the heat input and; consequently, to the material stress, the material flow, and the temperature in the stir zone. Yan *et al*. (2005) and Upadhyay and Reynolds (2010) observed an inverse relation between torque and temperature. For higher temperatures, the local stress in the material is lower and, consequently, the torque is lower. Moreover, torque can be used for the process control and to the proper selection of the equipment to carry out the FSW process (Su *et al*., 2013; Mehta *et al*., 2013). Khandkar *et al*. (2003); Schmidt *et al*. (2004) and Pew *et al*. (2007) computed the power in an FSW process as the torque multiplied by the rotational speed.

Considering the importance of the torque for the FSW process and weld quality, this quantity has been experimentally studied by several authors. Long *et al.* (2007); Yan *et al*. (2005); Pew *et al*. (2007); Leitao *et al*. (2012); Quintana and Silveira (2017a) observed experimentally the torque behavior as a function of the rotational and welding speeds. The studies showed that the rotational speed has more influence on the torque than the welding speed. However, a few authors have presented models for the torque behavior. Schmidt *et al.* (2004) considered three types of contact conditions in the tool-material interface to describe the torque: sticking condition, sliding condition and partial sticking/sliding condition when a combination of both conditions is present in the tool-material interface. The computed torque value was used to describe the heat input in the FSW. Pew *et al.* (2007) used the statistical software MINITAB to describe the torque behavior for aluminum alloys 7075, 5083, and 2024 based on experimental observations. The authors proposed statistical torque models for each material as a function of tool depth and rotational and welding speeds. Arora *et al.* (2009) developed a numerical model to explain the influence of rotational speed and tool geometry on the torque behavior. The model was based on the Mises criterion to describe yielding, and considered the yield stress as a function of temperature. Cui *et al.* (2010) proposed an experimental model to describe the torque for the aluminum

alloy 356 as an exponential function, and the function parameters were obtained based on experimental results for different rotational and welding speeds.

The inverse problem method has been widely used within the last few years to estimate parameters or functions in mathematical models using experimental data (Orlande, 2010). This method has been successfully applied in engineering, mainly in thermal engineering (Woodbury *et al.*, 2014; Barrios *et al.*, 2014). However, inverse or optimization methods have been rarely implemented to improve FSW models with respect to experimental data. Only a few studies in FSW have used the inverse problem method, and these were focused on heat transfer (Lambrakos *et al.*, 2003; Pereyra *et al.*, 2014). Taking into account that the exact expression to describe the torque behavior is still in development, the use of the inverse problem method to estimate parameters is an important tool to obtain a better and more accurate description. Moreover, based on both analyses, model and experiment, a better description of the problem is obtained.

In this paper, experimental data for the torque in FSW process are obtained at four levels for the rotational speed, namely, 600, 900, 1200, and 1500 rpm, and three levels for the welding speed, 100, 200, and 300 mm/min. The inverse problem method is implemented to estimate the parameters of an experimental torque model (Cui *et al.*, 2010). The experimental results are used as input data for the Levenberg–Marquardt method to estimate the parameters for the presented model. The optimized model obtained using the inverse problem method showed more consistent results.

2. EXPERIMENTAL PROCEDURE

The welds were carried out in a computer numerical control (CNC) machining center adapted to FSW. A fixture device was designed to guarantee a suitable arrangement of the specimens during the process. A Kistler 9272 dynamometer and a multichannel charge amplifier Kistler 5070 was used to measure the torque and for the signal conditioning, respectively. Figure 1 shows the CNC machining adapted to carry out the welds.

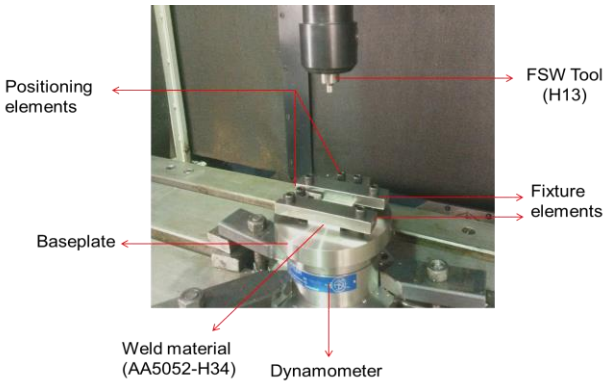

Figure 1. CNC machining adapted to the FSW process.

AA 5052-H34 specimens with a thickness of 5mm were joined by FSW at four levels of rotational speed ω (600, 900, 1200, and 1500 rpm) and three levels of welding speed v_w (100, 200, and 300 mm/min). For each pair of parameters, three replicas were performed. The tool material is H13 steel, heat treated to an average hardness of 50 HRC. The tool has shoulder and pin diameters of 10 and 4 mm, respectively, and a pin length of 4 mm. A total plunging depth of 4.1 mm and a plunging speed of 8 mm/min were kept constant for all the experiments. The dynamometer used in the experiments is able to measure the torque in its center; therefore, two groups of experiments were carried out to obtain the torque values for each phase, the first one for the plunging phase and the second one for the welding phase, during the steady state regime for the torque. Kumar *et al.* (2012) observed experimentally that the torque during the welding phase presents a steady state value.

3. INVERSE PROBLEM METHODOLOGY

The experimental model to describe the torque proposed by Cui *et al.* (2010) was selected to implement the inverse problem method and estimate the parameters. The criteria of selection were the easiness of the model and because it involves the main process variables, the rotational and welding speeds. However, tool geometry, material properties, and other variables are not considered. The model has the following form:

$$M = A + Bv_w + \left(C + Dv_w\right)e^{-(a+bv_w)\omega} \quad (1)$$

where v_w and ω are the welding and rotational speeds, respectively, and *A*, *B*, *C*, *D*, *a* and *b* are the parameters obtained experimentally. The model presents an exponential decay behavior of the torque as a function of the welding and rotational speeds. The parameters *A* and *B* correspond to the minimum torque values, *C* and *D* are the pre-exponential parameters, and *a* and *b* describe the decay function.

The inverse problem method used to estimate the model parameters followed the procedure described by Quintana and Silveira (2017b). The sensitivity coefficients, that represent the sensitivity of the torque in relation to the variation of the model parameters, were founded analytically by differentiating the model expressions with respect to each parameter. The analysis was performed with five different welding speeds: 100, 200, 300, 400, and 500 mm/min. The sensitivity coefficients were analyzed to evaluate their absolute values and the linear dependence between them. Small sensitivity leads to the same torque value being obtained for a wide range of values for the parameters, thus making parameter estimation difficult. On the other hand, the sensitivity coefficients cannot be expressed as a linear combination of each other to avoid problems with matrix singularity. In order to obtain better estimates, the parameters corresponding to sensitivity coefficients linearly independent were chosen to be estimated simultaneously, i.e., those parameters which are not expressed as a linear combination of each other and with large absolute values. For ease of comparison between the magnitude of the sensitivity coefficients and the analysis of linear dependence, reduced sensitivity coefficients were used as defined by Naveira-Cotta *et al.* (2010) as the product between the sensitivity coefficient and the parameter related to it.

The D-optimum design was used to select the optimal maximum rotational speed, and number of measurements for estimating the parameters by means of the variable and fixed frequency analysis, respectively. The Levenberg-Marquardt iterative method was implemented to estimate the parameters using the experimental data as input. Experimental results for the torque carried out with a welding speed of 300 mm/min at several rotational speeds were used to estimate the parameters. Considering that the estimation of the parameters by means of inverse problem require a large number of measurements and the complexity of obtaining experimental data for a wide range of rotational speeds, the trend curve of the experimental data obtained experimentally was used.

4. EXPERIMENTAL RESULTS

Figure 2 shows the torque as a function of time during the plunging phase (plunging of the tool into the material) for a rotational speed of 1500 rpm. The beginning of the plunging phase is in point 1, a stabilization period occurs in point 2, the effect of the shoulder on the torque value is observed at point 3 when the extruded material due to the penetration of the pin makes contact with the shoulder. The maximum torque value in the plunging phase, when the tool achieves the total plunging depth, is indicated in point 4. The torque during the welding phase (when the tool displaces to produce the weld) presents a steady state value (Kumar *et al.*, 2012) which is represented in Fig 2.

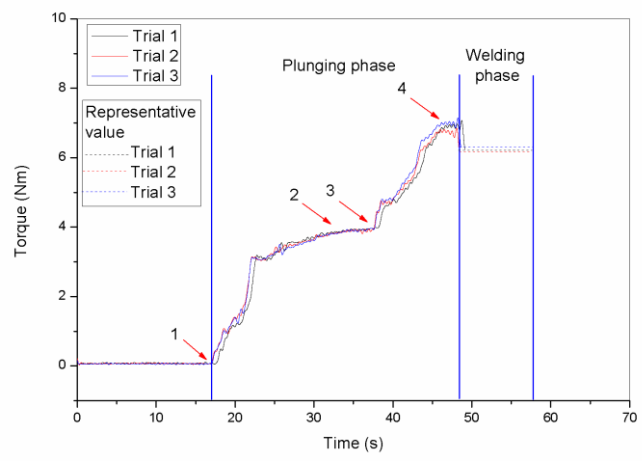

Figure 2. Torque as a function of time during the FSW experiment for a rotational speed of 1500 rpm.

Figure 3 shows the torque behaviour in FSW as a function of the rotational speed for all the welding speeds during the plunging and the welding phases. The results show that, the torque value is higher during the plunging phase, nevertheless, for higher rotational speeds the difference between the torque in the plunging and welding phases is

smaller. Additionally is observed that the increase of the rotational speed decreases the torque value. Higher rotational speeds produce an increment of the local temperature in the material and consequently, the local yield stress of the material decreases and the torque value also decreases (Yan *et al.*, 2005; Upadhyay *et al.*, 2010). On the other hand, the influence of the welding speed on the torque is significantly smaller than the influence of the rotational speed; during the plunging phase, the welding speed does not have influence on the torque value, however, during the welding phase the torque is influenced by the interaction of the welding speed and the rotational speeds. For higher rotational speeds, the influence of the welding speeds on the torque during the welding phase is smaller. The high heat input to the process owing to the higher rotational speeds diminished the local yield stress of the material and under these conditions, the welding speed present a smaller influence on the torque. The analysis of variance (ANOVA), presented in Table 1 confirm this behavior. The statistical analysis indicates that for a statistic F of 3.29 and a p-level of 0.0167, there is an interaction between the effects of rotational and welding speeds factors on the torque during the welding phase.

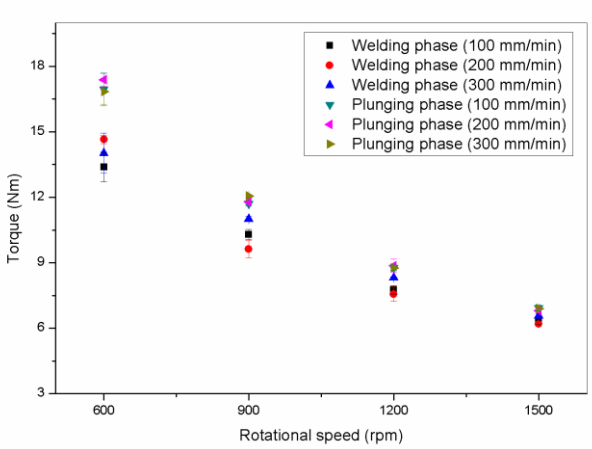

Figure 3. Torque as a function of the rotational speed for all the welding speeds during the plunging and welding phases.

Table 1. Analysis of variance (ANOVA) for the torque during the welding phase

Source	Degree of freedom	Sum. Sq.	Mean Sq.	F	p-level
ω	3	302.802	100.934	465.3	0
v_w	2	2.166	1.083	4.99	0.0154
$\omega \cdot v_w$	6	4.277	0.713	3.29	0.0167
Erro	24	5.206	0.217		
Total	35	314.451			

As observed in Fig. 3, the torque has an exponential decay behavior as a function of the rotational speed, for all the experiments. Table 2 presents the fitted equations for the torque at each welding speed during the welding phase and for the torque during the plunging phase. In all cases, the fitted equation is a downward exponential function for the torque as a function of the rotational speed.

Table 2. Fitted equations for torque as a function of the rotational speed.

Welding speed (mm/min)	Fitted curve equation	Data fitting correlation (R^2)
Plunging phase		
---	$M = 30.298e^{-1\times10^{-3}\omega}$	0.992
Welding phase		
100	$M = 22.195e^{-9\times10^{-4}\omega}$	0.997
200	$M = 24.231e^{-9\times10^{-4}\omega}$	0.968
300	$M = 23.435e^{-9\times10^{-4}\omega}$	0.999

5. ESTIMATION OF PARAMETERS VIA INVERSE PROBLEM

The sensitivity coefficients computed analytically for each model parameter and the linear dependence between them are presented in Table 3. The results shows that, for a constant welding speed exist linear dependence between sensitivity coefficients of parameters *A* and *B*, *C* and *D*, and *a* and *b*. Figure 4 shows the reduced sensitivity coefficients behavior as a function of the rotational speed. According to the results from Table 3, in Fig 4 is observed that the reduced sensitivity coefficients J_A and J_B present a constant and small value, indicating linear dependence. The reduced sensitivity coefficient J_D presents a constant and small value after approximately 700 rpm and a linear dependence with respect to J_C. The reduced sensitivity coefficients related to the parameters *a* and *b* are also linearly dependent as indicated in Table 3. Therefore, considering the magnitude of the sensitivity coefficients and the linear independence between them, only the parameters *A*, *C*, and *a* are estimated via inverse problem. The other parameters were assumed with the same value as the original experimental value proposed by Cui *et al.* (2010).

Table 3. Sensitivity coefficients for the parameters of the experimental model.

Model parameter	Sensitivity coefficient	Linear Dependence between the sensitivity coefficient
A	$J_A = \frac{\partial M}{\partial A} = 1$	LD with respect to J_B
B	$J_B = \frac{\partial M}{\partial B} = v_w$	LD with respect to J_A
C	$J_C = \frac{\partial M}{\partial C} = e^{-(a+bv_w)\omega}$	LD with respect to J_D
D	$J_D = \frac{\partial M}{\partial D} = v_w e^{-(a+bv_w)\omega}$	LD with respect to J_C
a	$J_a = \frac{\partial M}{\partial a} = -\left(C + Dv_w\right) e^{-(a+bv_w)\omega}$	LD with respect to J_b
b	$J_b = \frac{\partial M}{\partial b} = -v_w \omega \left(C + Dv_w\right) e^{-(a+bv_w)\omega}$	LD with respect to J_a

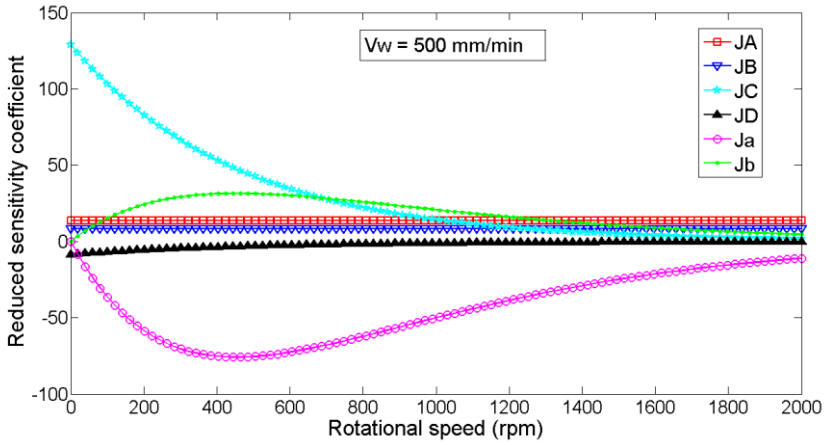

Figure 4. Reduced sensitivity coefficients for a welding speed of 500 mm/min

The D-optimum design for variable and fixed frequencies is shown in Fig. 5a and 5b where a maximum rotational speed of approximately 1500 rpm and 1000 measurements are identified as optimal in the variable and fixed frequency analysis, respectively. Moreover, the variable frequency shows higher absolute values for higher welding speeds while the fixed frequency analysis shows a similar behavior for all the welding speeds.

Considering the sensitivity coefficients analysis, the estimation of parameters was carried out for a maximum rotational speed of 1500 rpm, 1000 measurements and the experimental data of torque obtained with a welding speed of 300 mm/min. The initial values for the parameters were the original values proposed by Cui *et al.* (2010). Figure 6a

shows the convergence of the Levenberg–Marquardt method for the estimated parameters: *A=3.0222*, *C=83.9655*, and *a=0.0053*. Figure 6b presents a comparison between the experimental data for torque, the original Cui's model, and the model with the estimated parameters. The model for the torque using the estimated parameters presented results with better agreement to the experimental data than using the original Cui's model (Cui *et al.*, 2010). Table 4 presents the relative error between the experimental data and both models, original Cui's model and adjusted model via inverse problem.

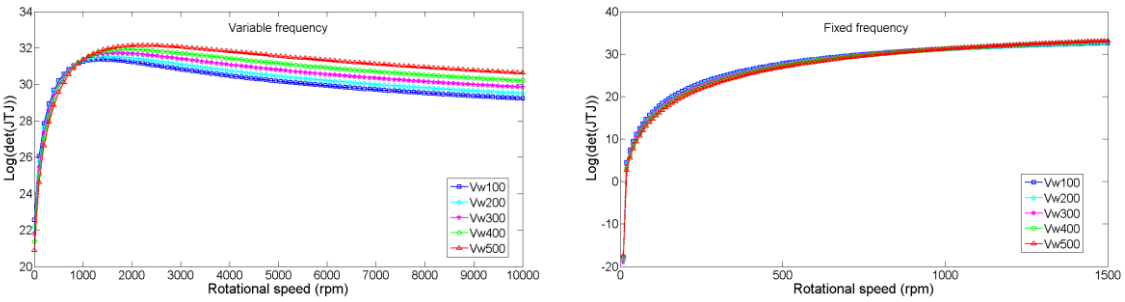

a) b)

Figure 5. a) Variable and b) fixed frequencies for all the welding speeds.

Some variables of the FSW process not considered in the original model, such as tool geometry and material properties could be related to the differences between the estimated model using inverse problem methodology and the original model. Khandkar *et al.* (2003) and Schmidt *et al.* (2004) determined that the value of the torque in the FSW process involves the tool geometry and the properties of the weld material. The original Cui´s model (Cui *et al.*, 2010). were obtained from experimental data for torque using a tool with a shoulder diameter of 18 mm and a pin diameter of 6 mm whereas the experimental data using in this work to estimate the parameters of the model presented in Eq. 1 were carried out using a tool with 10 mm of shoulder diameter and 4 mm of pin diameter. Additionally, the weld material in the both cases is different; the original Cui´s model (Cui *et al.*, 2010) was obtained for A356 cast aluminum alloy and for the adjusted of the model was used 5052-H34 aluminum alloy. However, the implementation of the inverse problem methodology can be a successful tool to adjust this model for different aluminum alloys and tool geometries as showed in Figure 5b and in the relative error presented in Table 4.

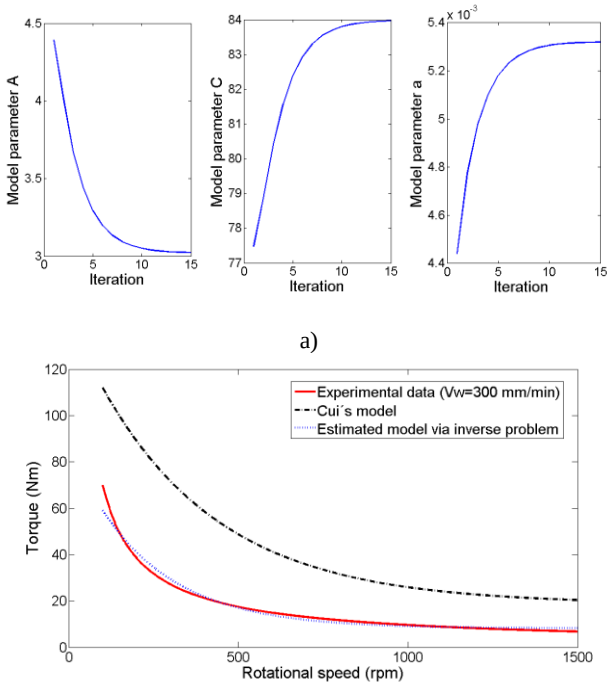

a)

b)

Figure 6. a) Levenberg-Marquardt convergence for the estimated parameters, b) Comparison between the experimental data for a welding speed of 300 mm/min, the original model (Cui *et al.*, 2010) and the estimated model via inverse problem.

Table 4. Relative error for the Cui´s experimental model and the adjusted model via inverse problem in relation to the experimental data for torque.

Rotational speed (rpm)	Relative error (%)	
	Adjusted model via IP	Cui´s experimental model
600	2.3	176.7
900	17.2	169.1
1200	19.6	177.2
1500	0.0	273.2

6. CONCLUSIONS

The experimental results for the torque at different rotational and welding speeds showed that the rotational speed has a higher influence on the torque than the welding speed. The torque presented an exponential decay with the rotational speed while it presented a slight increase with the increment of the welding speed. The variance analysis showed that there is an interaction between the effects of rotational and welding speeds on the torque during the welding phase, suggesting that the influence of these factors on the torque in the welding phase must be analyzed together. On the other hand during the plunging phase, the torque presents a higher value, mainly for lower rotational speeds, which is not influenced by the welding speeds.

The inverse problem method was implemented successfully to adjust an experimental model for the torque behavior by means of the Levenberg-Marquardt iterative method for the estimation of parameters. The linear dependence between the model parameters does not allow for estimating all the model parameters. Only three parameters can be estimated; however, the presented model with new parameters values has a better agreement with the torque experimental data.

The differences between the original Cui's model and the model estimated via inverse problem are related to the influence of the other factors, not considered in the original model, on the torque, such as the tool geometry and material properties.

7. ACKNOWLEDGEMENTS

This work was partially supported by CAPES, the Brazilian Federal Agency for Support and Evaluation of Graduate Education; CNPq, the Brazilian National Council for Scientific and Technological Development and FAPERJ, the Foundation for Research Support of the State of Rio de Janeiro, Brazil.

8. REFERENCES

Arora A., Nandan R., Reynolds A. and DebRoy P., 2009. "Torque, Power Requirement and Stir Zone Geometry in Friction Stir Welding Through Modeling and Experiments". *Scripta Materialia*, Vol. 60, p. 13-16.

Barrios A.N.S., Silva J.B.C, Rodrigues A.R., Coelho R.T., Braghini Junior A. and Matsumoto H., 2014. "Modeling heat transfer in die milling". *Applied Thermal Engineering*, Vol. 64, p. 108-116.

Cui, S., Chen Z.W. and Robson J.D., 2010. "A model relating tool torque and its associated power and specific energy to rotation and forward speeds during friction stir welding/processing". *International Journal of Machine Tools and Manufacture*, Vol. 50, p. 1023-1030.

Khandkar M., Khan J. and Reynolds A., 2003. "Prediction of temperature distribution and thermal history during friction stir welding: input torque based model". *Science and Technology of Welding and Joining*, Vol. 8, p. 165-174.

Kumar R., Singh K. and Pandey S., 2012. "Process forces and heat input as function of process parameters in AA5083 friction stir welds". *Transactions of Nonferrous Metals Society of China*, Vol. 22, p. 288-298.

Lambrakos S.G., Fonda R.W., Milewski J.O. and Mitchell J.E., 2003. "Analysis of friction stir welds using thermocouple measurements". *Science and Technology of Welding and Joining*, Vol. 8, p. 385-390.

Leitao C., Louro R. and Rodrigues D.M., 2012. "Using Torque Sensitivity Analysis in Accessing Friction Stir Welding/Processing conditions". *Journal of Materials Processing Technology*, Vol. 212, p. 2051-2057.

Long T., Tang W. and Reynolds A., 2007. "Process Response Parameter Relationships in Aluminium Alloy Friction Stir Welds". *Science and Technology of Welding and Joining*, Vol. 12, p. 311-317.

Mehta M., Chatterjee K. and De A., 2013. "Monitoring torque and traverse force in friction stir welding from input electrical signatures of driving motors". *Science and Technology of Welding and Joining*, Vol. 18, p. 191-197.

Mishra R.S and Ma Z.Y., 2005. “Friction Stir Welding and Processing”. *Materials Science and Engineering R*, Vol. 50, p. 1-78.

Naveira-Cotta C.P., Cotta R.M., Orlande H.R.B. and Kakaç S., 2010. “Direct and inverse problems solutions in micro-scale forced convection”. In *Microfluidics Based Microsystems, NATO Science for Peace and Security Series A: Chemistry and Biology*, Springer, Dordrecht, The Netherlands, p. 39-59.

Orlande, H.R.B., 2010. “Inverse problems in heat transfer: New trends on solution methodologies and applications”. *ASME Journal of Heat Transfer*, Vol. 134, p. 031001.

Pereyra S., Lombera G.A. and Urquiza S.A., 2014. “Modelado numérico del proceso de soldadura FSW incorporando una técnica de estimación de parámetros”. *Revista Internacional de Métodos Numéricos para Cálculo y. Diseño en Ingenieria*, Vol. 30, p. 173-177.

Pew J.W., Nelson T.W. and Sorensen C.D., 2007. “Torque based weld power model for friction stir welding”. *Science and Technology of Welding and Joining*, Vol. 12, p. 341-347.

Qian J., Li J., Sun F., Xiong J., Zhang F. and Lina X., 2013. “An analytical model to optimize rotation speed and travel speed of friction stir welding for defect-free joints”. *Scripta Materialia*, Vol. 68, p. 175-178.

Quintana K.J and Silveira J.L., 2017a. “Mechanistic models and experimental analysis for the torque in FSW considering the tool geometry and the process velocities”. *Journal of Manufacturing Processes*, Vol. 30, p. 406-417.

Quintana K.J and Silveira J.L., 2017b. “Analysis of Torque in Friction Stir Welding of Aluminum Alloy 5052 by Inverse Problem Method”. *ASME Journal of Manufacturing Science and Engineering*, Vol. 139, p. 041017.

Rajakumar S., Muralidharan C. and Balasubramanian V., 2011. “Statistical Analysis to Predict Grain Size and Hardness of the Weld Nugget of Friction Stir Welded AA6061-T6 Aluminium Alloy Joints”. *International Journal of Advanced Manufacturing Technology*, Vol. 57, p. 151-165.

Rhodes C.G., Mahoney M.W., Bingel W.H., Spurling R.A. and Bampton C.C., 1997. “Effects of Friction Stir Welding on Microstructure of 7075 Aluminum”. *Scripta Materialia*, Vol. 36, p. 69-15.

Schmidt H., Hattel J. and Wert J., 2004. “An analytical model for the heat generation in friction stir welding”. *Modelling and Simulation in Materials Science and Engineering*, Vol. 12, p. 143-157.

Su H., Wu C.S., Pittner A. and Rethmeier M., 2013. “Simultaneous measurement of tool torque, traverse force and axial force in friction stir welding”. *Journal of Manufacturing Processes*, Vol. 15, p. 495-500.

Upadhyay P. and Reynolds A.P., 2010. “Effects of Thermal Boundary Conditions in Friction Stir Welded AA7050-T7 Sheets”. *Materials Science and Engineering A*, Vol. 527, p. 1537-1543.

Woodbury K.A., Beck J.V. and Najafi H., 2014. “Filter solution of inverse heat conduction problem using measured temperature history as remote boundary condition”. *International Journal of Heat and Mass Transfer*, Vol. 72, p. 139-147.

Yan J., Sutton M. and Reynolds A., 2005. “Process-structure-property relationships for nugget and heat affected zone regions of AA2524-T351 friction stir welds”. *Science and Technology of Welding and Joining*, Vol. 10, p. 725-736.

9. RESPONSIBILITY NOTICE

The authors are the only responsible for the printed material included in this paper.